Probabilistic and Deterministic Semi-Active Control Strategies for Adjacent Buildings Connected by MR Dampers

Sasan. Babaei[1], Panam. Zarfam[2], Abdolreza. Sarvghad Moghadam[3]

[1] *Student, Department of Civil Engineering, Science and Research Branch, Islamic Azad University, Tehran 14778-93855, Iran., sasan.babaei@srbiau.ac.ir*

[2] *Professor, Department of Civil Engineering, Science and Research Branch, Islamic Azad University, Tehran 14778-93855, Iran., zarfam@srbiau.ac.ir*

[3] *Professor, Structural Engineering Research Center, International Institute of Earthquake Engineering and Seismology, Tehran 19537-14453, Iran., moghadam@iiees.ac.ir*

Abstract

A semi-active control system can reduce the seismic response with proper reliability and requires a small external power source with which to operate. The use of magnetorheological (MR) dampers for semi-active control of structures has recently increased, especially to address pounding in adjacent high-rise buildings. An MR damper provides a large damping force, fast response, and simplicity of design. Previous research has investigated design optimization, the efficacy of the control algorithms, self-powered and energy-saving technologies and integration of different control systems. However, these studies have not addressed the random characteristics of structural systems. The current study investigated the performance levels of 10- and 20-story linear coupled shear-type model buildings connected by MR dampers in the time domain. Numerical computation was performed in MATLAB. The mass of the floors was assumed to be concentrated at their centers and the structural modes were well-separated. The modified Bouc-Wen model was employed to model the hysteretic behavior of the MR damper. Two sets of ground motions were used, one comprising 40 records taken from a FEMA project at a hazard level of 2 and a 10% probability of exceedance in 50 years and the other comprising 22 far-field records suggested by FEMA P695. The effectiveness of the linear quadratic regulator, Lyapunov and simple adaptive control (SAC) have been compared. In SAC, the response is optimized by forcing the controlled structure to behave like the reference model with the desired trajectories. The computation of adaptive gains does not require explicit system identification or observation. The performance levels of the buildings were initially calculated using the Hazus recommendations for each algorithm and ground motion. Inter-story drift and floor acceleration were the performance measures. The seismic fragility curves of both uncontrolled and controlled 20- story buildings were obtained for 22 records using incremental dynamic analysis (IDA). Finally, uncertainty in the structural characteristics was expressed in the mass, stiffness, and damping of the floors. Monte Carlo analysis was combined with IDA to determine the probability of meeting or exceeding each damage state (slight, moderate, extensive and complete). Although the structural behavior was record-dependent, the numerical simulations showed that all algorithms coupled with the MR damper were effective for response reduction of buildings subjected to a range of external excitation. SAC was more effective in reducing inter-story drift and peak absolute acceleration, especially when subjected to records with higher intensity. In the presence of uncertainty, SAC also yielded higher coefficients for ground acceleration at each performance level.

Keywords: Adjacent buildings, Semi-active control, MR damper, Probabilistic analysis, Performance-based design

Introduction

Seismic risk reduction of high-rise buildings, particularly adjacent structures, is increasingly intertwined with control strategies. Coupling two structures with a damper is one method that generates a period shift, dissipates energy, provides evacuation corridors at the connecting elements, and decreases the damage caused by pounding.

The need for a severe power supply and the probability of structural instability in active control, has prompted an increase in studies on semi-active control, which uses a limited amount of energy to adjust the dynamic characteristics of the system. Semi-active control comprises a range of dampers, including a variable orifice, adjustable tuned liquid, variable stiffness, and controllable fluid dampers[1]. The magnetorheological (MR) damper is robustly grown in structural control and can provide a high level of energy at lower voltage, has fast control response, simplicity of design and passive control during a power cut or control algorithm.

Studies have investigated energy harvesting systems[2], design or damper orientation optimization and hybrid control strategies regarding these dampers. The use of advanced control methods such as fuzzy logic and genetic algorithms[3] have been compared with traditional algorithms such as the linear quadratic regulator, LQG and Lyapunov-based algorithms, sliding mode control and PID[4]. Simple adaptive control (SAC) is a control algorithm in which the control structure is forced to follow an ideal reference model. This type of direct adaptive control was first introduced by Sobel et al.[5] and was later updated by Barkana[6] and Kauffman[7]. This algorithm performs suitably in the presence of uncertainty.

Uncertainty in coupled systems with MR dampers has only been investigated through the presence of noise and defects in low rise buildings[8, 9]. Few studies have addressed uncertainty in high-rise buildings. To this end, the performance of a structure has been evaluated using three control methods and their results were compared when subjected to 40 records at a hazard level of 2 and a 10% probability of exceedance. Fragility curves of a structure controlled using the SAC method have been compared with those of an uncontrolled structure. The probability of damage has been evaluated using Monte Carlo analysis.

System description

Two adjacent buildings with different dynamic properties were modeled in a linear shear-type model. The mass was concentrated in the center of the floors and the two structures were connected at the floors. The first structure had $n_1 + 2n_2$ degrees of freedom (DoF) and the second structure had n_2 DoF from the sum of $n_1 + 2n_2$ DoF as presented in Fig. 1. The MR damper was used to control the system by rigidly connecting the structures at the floors. Any effect of soil on the structure was neglected and the plans of the structures were considered to be symmetric. The matrix equation of the structural system motion can be written as:

$$[M]\{\ddot{x}(t)\} + [C]\{\dot{x}(t)\} + [K]\{x(t)\} = [J]\{f_m(t)\} - [M][\Lambda]\ddot{x}_g(t) \tag{1}$$

where M, K, and C are the mass, stiffness and damping matrices of the coupled system, f_m is the MR damper force vector, and J is the matrix that defines the location of the control forces. The mass and stiffness matrices can be expressed as:

$$M_{(n1+2n2,n1+2n2)} = \begin{bmatrix} M_{1(n_1,n_2,n_1,n_2)} & 0_{(n_1,n_2,n_2)} \\ 0_{(n_2,n_1,n_2)} & M_{2(n_2,n_2)} \end{bmatrix} \tag{2}$$

$$K_{(n1+2n2,n1+2n2)} = \begin{bmatrix} K_{1(n1+n2,n1+n2)} & 0_{(n1+n2,n2)} \\ 0_{(n_2,n_1,n_2)} & K_{2(n_2,n_2)} \end{bmatrix} \tag{3}$$

$$C_{(n1+2n2,n1+2n2)} = \begin{bmatrix} C_{1(n1+n2,n1+n2)} & 0_{(n1+n2,n2)} \\ 0_{(n2,n1+n2)} & C_{2(n_2,n_2)} \end{bmatrix} \tag{4}$$

where M_1, M_2, K_1, K_2, C_1, and C_2 are the mass, stiffness, and damping of each unconnected building.
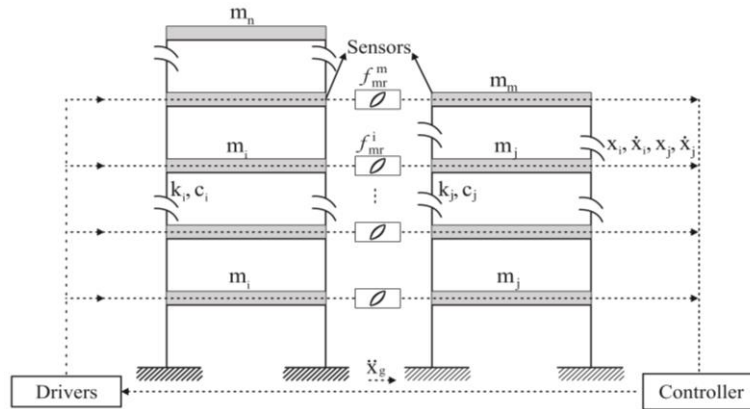
2

Fig. 1. Shear buildings with MR dampers[3].

The system state equation can be written as[10]:

$$\dot{y} = Ay + Bf_m(t) + E\ddot{x}_g(t) \tag{5}$$

where y, A, B, E are the state vector, system matrix, control force distribution matrix and excitation, respectively, and can be evaluated as:

$$y = \begin{Bmatrix} \{x\} \\ \{\dot{x}\} \end{Bmatrix} \tag{6}$$

$$A = \begin{bmatrix} [0] & [I] \\ (n_1 + 2n_2, n1 + 2n_2) & (n_1 + 2n_2, n1 + 2n_2) \\ -[M]^{-1}[K] & -[M]^{-1}[C] \end{bmatrix} \tag{7}$$

$$B = \begin{Bmatrix} [0] \\ (n_1 + 2n_2, n1 + 2n_2) \\ [M]^{-1}[J] \end{Bmatrix} \tag{8}$$

$$E = \begin{Bmatrix} \{0\} \\ (n_1 + 2n_2, 1) \\ \{-\Lambda\} \\ (n_1 + 2n_2, 1) \end{Bmatrix} \tag{9}$$

where ^ is a vector made up of elements equal to one.

Linear quadratic regulator

A linear quadratic regulator (LQR) is a classic, simple and well-known method of optimal control. The control vector should be calculated to minimize the quadratic cost function as[10]:

$$J_{lqr} = \int_0^\infty \{x_P(t)^T Q_{lqr} x_P(t) + u_P^T(t) R_{lqr} u_P(t)\} dt \tag{10}$$

The magnitude of decrease in the state variables and the control forces are balanced by weighting matrices Q_{lqr} and R_{lqr}. The values selected to tune the results were:

$$Q_{lqr} = \frac{1}{2} \begin{bmatrix} K & 0 \\ 0 & M \end{bmatrix} \tag{11}$$

$$R_{lqr} = \rho I_{(n1+2n2,n1+2n2)}; \; \rho = 1 \times 10^{-7.2} \tag{12}$$

3

Simple adaptive controller

In this method, the response is optimized by forcing the controlled structure to behave like the reference model with the desired trajectories. The control force is determined by the feedback error between the plant and the reference model. Computation of the adaptive gains does not require explicit system identification or observation. The linear equation governing the reference model and the plant are[11]:

$$\dot{x}_P(t) = A_P x_P(t) + B_P u_P(t) + d_i(t) \tag{13}$$

$$y_P(t) = C_P x_P(t) + D_P u_P(t) + d_o(t) \tag{14}$$

$$\dot{x}_m(t) = A_m x_m(t) + B_m u_m(t) \tag{15}$$

$$y_m(t) = C_m x_m(t) + D_m u(t) \tag{16}$$

The error and the control command are:

$$e_y(t) = y_m(t) - y_P(t) \tag{17}$$

$$u_P(t) = K(t) r(t) \tag{18}$$

where r(t) is the reference vector and is equal to:

$$r^T(t) = \left[\left(y_m(t) - y_P(t)\right)^T x_m^T(t) u_m^T(t)\right] \tag{19}$$

K(t) is the gain matrix made up of the integral and proportional gains, which are[11, 12]:

$$K(t) = K_I(t) + K_P(t) \tag{20}$$

$$\dot{K}_I(t) = e_y(t) r(t)^T T - \sigma K_I(t) \tag{21}$$

$$K_P(t) = e_y(t) r(t)^T T \tag{22}$$

in which T and T⁻ are tuning matrices which should be optimized by the operator to modify the adaptation rate. The σ-term contains small values and is used to prevent divergence in the results of the equation. Fig. 2 shows a block diagram representing the adaptive control system.

Fig. 2. Block diagram of simple adaptive controller[8].

Lyapunov stability theory-based algorithm

Lyapunov theory of stability is a direct control strategy in a feedback controller design. A positive definite Lyapunov function of the states of the system should be used to control the stability of the system. One function previously used by Leitmann is[13]:

$$L(y) = \frac{1}{2} \|x_P(t)\|_P \tag{23}$$

where the P-norm of the system state is equal to:

$$\|x_P(t)\|_P = [x_P(t)^T P_L x_P]^{1/2} \tag{24}$$

P_L in Eq. (24) is a real, symmetric, positive definite matrix governed by the following equation:

$$A_P^T P_L + P_L A_P + Q_L = 0 \tag{25}$$

in which Q_L is a positive definite matrix that can be selected.

The derivative of the Lyapunov function of the solution of state-space and the control law which will minimize it are:

$$\dot{L}(y(t)) = -\frac{1}{2} x_P(t)^T Q_L x_P(t) + x_P(t)^T P_L B f_m(t) + x_P(t)^T P_L E \ddot{x}_g(t) \tag{26}$$

$$v_i = V_{max} H\left(-x_P(t)^T P_L B\, f_m(t)\right) \tag{27}$$

where H(.) is the Heaviside function. This equation establishes that the control voltage is either V_{max} or zero.

Magneto-rheological damper

The Bouc-Wen model initially was used by Spencer et al. to predict the behavior of an MR damper. It then was modified by Spencer to accommodate nonlinearity more accurately[14]. The model depicted in Fig. 3 accommodates an extra dashpot and a spring to compensate for defects in model prediction at low velocities and the effect of the gas chamber[15].
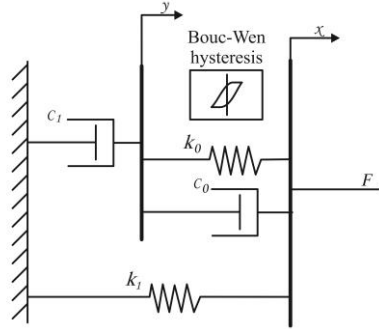
Fig. 3. Modified Bouc-Wen model for MR damper[11].

The damping force of the MR damper is given by[14]:

$$f_{mr}^i = C_1 \dot{y}_1 + K_1(X_{i+n} - X_i - X_0) \tag{28}$$

where y_i is the internal pseudo-displacement and z_{di} is the evolutionary variable.

$$\dot{y}_1 = \frac{1}{(C_0 + C_1)} \{\alpha z_{di} + C_0(\dot{x}_{n+i} - \dot{x}_i) + K_0(X_{n+i} - X_i - y_i)\} \tag{29}$$

$$\dot{z}_{di} = -\gamma|\dot{x}_{n+i} - \dot{x}_i - \dot{y}_i|z_{di}|z_{di}|^{n_d-1} - \beta(\dot{x}_{n+i} - \dot{x}_i - \dot{y}_i)|z_{di}|^{nd} + A_c(\dot{x}_{n+i} - \dot{x}_i - \dot{y}_1) \tag{30}$$

where x_i is the displacement of the ith floor, K_0 and k_1 are the accumulator stiffness and the stiffness at large velocities, respectively, and x_0 is the initial displacement of spring k_1. The viscous damping observed at higher and lower velocities are denoted by c_0 and c_1, respectively, and α is an evolutionary coefficient.

$$\alpha = \alpha_a + \alpha_b u; \ C_1 = C_{1a} + C_{1b}u; \ C_0 = C_{0a} + C_{0b}u \tag{31}$$

where u is the output of the following first-order filter:

$$\dot{u} = -\eta(u - v_i) \tag{32}$$

5

and v_i is the command input voltage of the damper on the ith floor. The parameters of the Bouc-Wen phenomenological model for the 1000 kN MR damper are presented in Table 1.

Table 1 - Parameters of Bouc-Wen phenomenological model for 1000 kN MR dampers[3].

Parameter	Value	Parameter	Value
c_{0a}	50.30 kN sec/m	α_a	8.70 kN/m
c_{0b}	48.70 kN sec/m/V	α_b	6.40 kN/m/V
k_0	0.0054 kN/m	γ	496.0 m^{-2}
c_{1a}	8106.2 kN sec/m	β	496.0 m^{-2}
c_{1b}	7807.9 kN sec/m/V	A_c	810.50
k_1	0.0087 kN/m	n_d	2
x_0	0.18 m	η	195 sec^{-1}

Numerical example

The coupled system comprised two 20- and 10-story structures as developed by Bharti et al. that were connected by a rigid connection of MR dampers[16]. The mass and stiffness of the two structures were 800 tons and 1.4×10^6 kN/m, respectively. The dominant periods of the two structures were well separated and the first periods of the structures were 1.96 and 1.005. Typical Rayleigh damping of 5% was considered in the analysis. The height of the floors was 3.2 m.

Results and discussion

The semi-active control of the structures was analyzed using three algorithms under 40 seismic records taken from the FEMA/SAC project at a hazard level of 2 and a 10% probability of exceedance in 50 years[17]. Roof displacement, interstory drift, and floor acceleration were the performance measures used. These performance criteria are evaluated as[18]:

$$J_1 = \frac{\max(|x_i(t)|)}{x_{unctrl}} \tag{33}$$

$$J_2 = \frac{\max(|d_i(t)|)}{d_{unctrl}} \tag{34}$$

$$J_3 = \frac{\max(|\ddot{x}_i(t)|)}{\ddot{x}_{unctrl}} \tag{35}$$

where J_1, J_2, and J_3 are the displacement, acceleration, and drift criteria that establish the efficiency of the control strategies. Hazus recommendations were used to evaluate the structural performance as presented in Table 2.

Table 2- Structural performance levels for reinforced concrete moment-resisting frames[19].

Interstory drift at threshold of damage state			
Slight	Moderate	Extensive	Complete
0.0025	0.0050	0.0150	0.04

Figs. 4 and 5 show the maximum roof displacement under the 1992 Yermo Landers (LA10) and 1974 Tabas (LA30) ground motions. Although the Lyapunov control algorithm did not initially show a significant decrease in response, it subsequently reduced the peak roof displacement. The SAC control algorithm, on the other hand, by following the ideal LQR model, significantly reduced the response, especially when subjected

6

to the LA30 record (41%). The roof acceleration of the 20-story building presented in Figs. 6 and 7 show a drop when utilizing the LQR and SAC methods. These reductions were much less than those for displacement and were 8% and 12%, respectively, under SAC. The Lyapunov control algorithm had an adverse effect and increased the peak acceleration to 3% for LA10.

Interstory drift in the 20-story building is shown in Fig. 8. Unwelcome rotation in the lower floor columns was reduced almost by half, especially for the LA30 seismic, at 47% for SAC and 19% for Lyapunov. Table 3 shows the performance criteria results and reveals the prominent response reduction for SAC in comparison with Lyapunov, especially when subjected to ground motions with a 2% probability of exceedance. This method reduced the peak roof displacement and interstory drift of the uncontrolled structure by 37% and 35%, respectively.
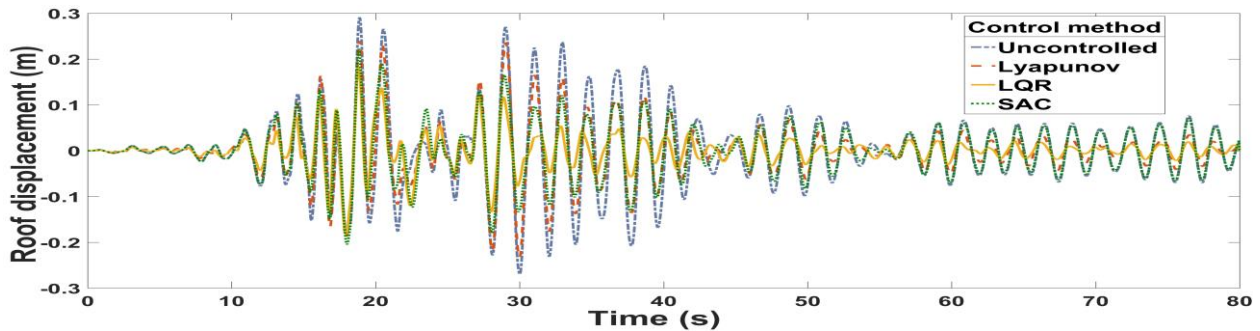
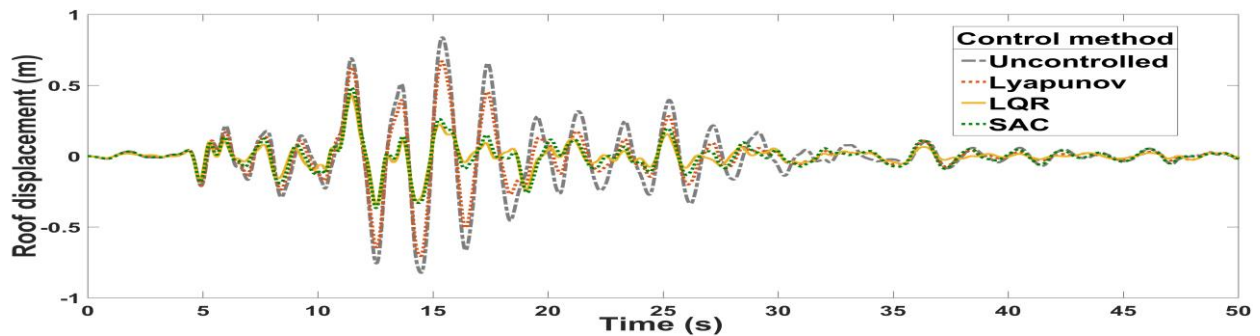Fig. 4. Roof displacement time history of the 20- story building under LA10 seismic record

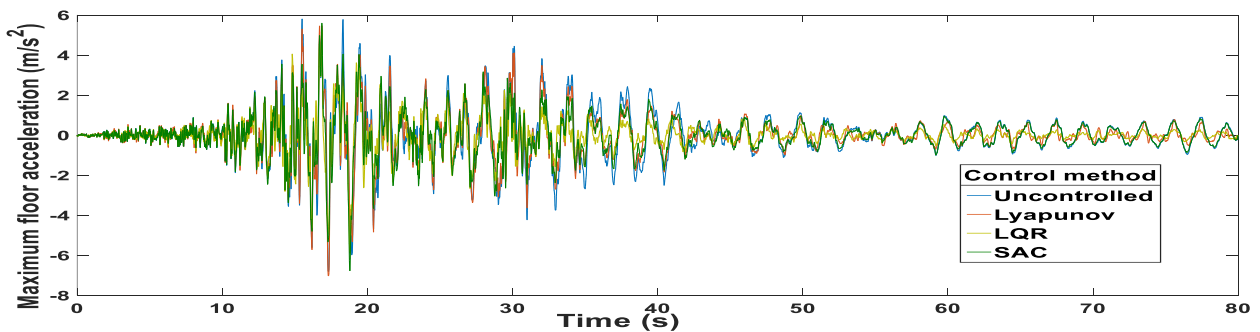Fig. 5. Roof displacement time history of the 20- story building under LA30 seismic record.

Fig. 6. Roof acceleration time history of the 20- story building under LA10 seismic record.
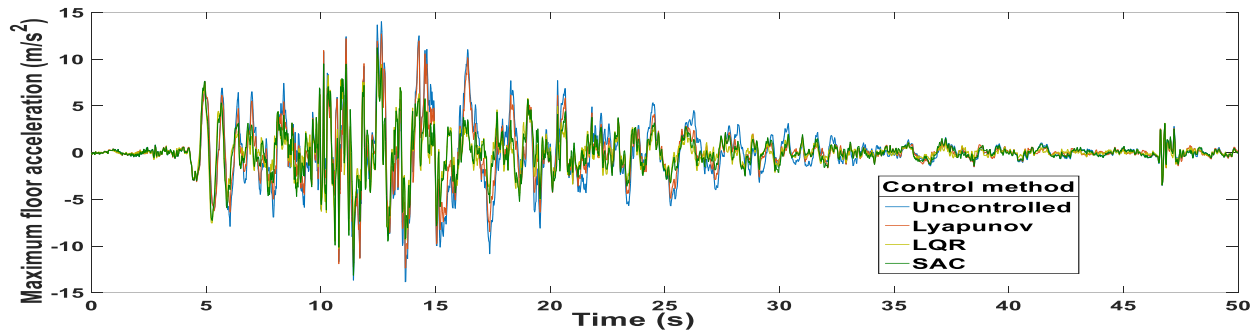
7

Fig. 7. Roof acceleration time history of the 20- story building under LA30 seismic record.
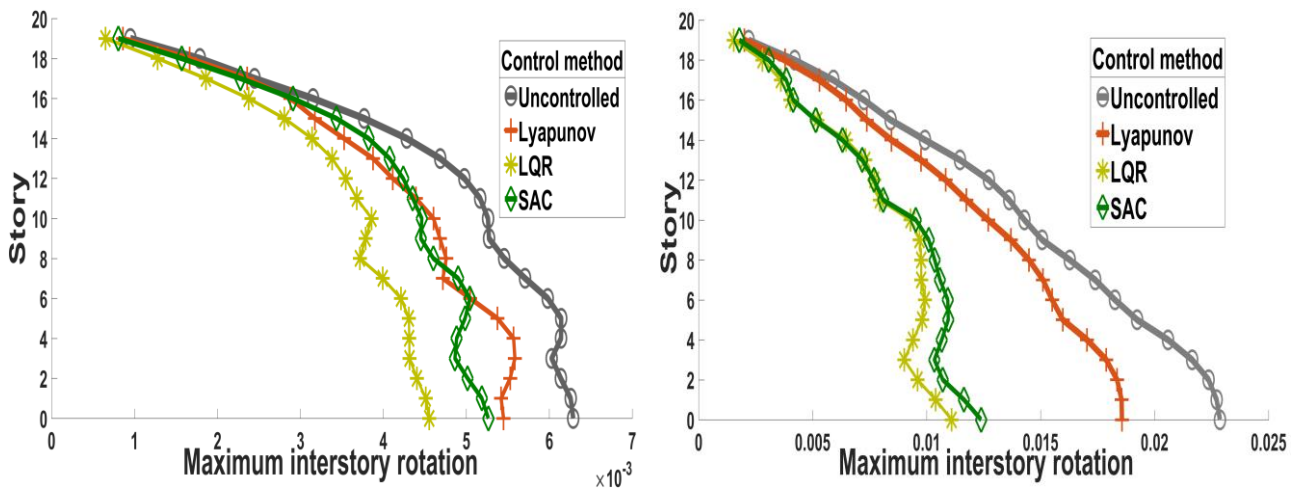

Fig. 8. Peak interstory drift of the 20- story building under; a) LA10, b) LA30 seismic record.

Table 3 - Evaluated performance indices due to various earthquake excitations.

Seismic record	Control method	J_1		J_2		J_3	
LA10	Lyapunov	0.82		0.89		1.03	
	LQR	0.63		0.73		0.86	
	SAC	0.74		0.84		0.94	
LA30	Lyapunov	0.84		0.81		0.90	
	LQR	0.52		0.48		0.83	
	SAC	0.59		0.53		0.88	
		M	SD	M	SD	M	SD
LA01-LA20	Lyapunov	0.9184	0.0752	0.9004	0.0543	0.9831	0.0296
	LQR	0.5987	0.1047	0.5918	0.1048	0.9092	0.1245
	SAC	0.6781	0.1083	0.7086	0.1233	0.9746	0.1709
LA21- LA40	Lyapunov	0.9186	0.0454	0.8956	0.0441	0.9700	0.0423
	LQR	0.5608	0.0868	0.5548	0.0875	0.8254	0.1305
	SAC	0.6305	0.1148	0.6476	0.0932	0.8124	0.1662

M: mean (m/s2), SD: standard deviation

8

The fragility curves for the 20-story building controlled by the SAC algorithm were developed using incremental dynamic analysis (IDA) of 22 far-field records[20, 21] and are presented in Fig. 9. The uncontrolled fragility curves that consider interstory drift are also shown. This lognormal diagram indicates that the extensive and complete damage states were exceeded by uncontrolled structures when the average peak ground acceleration of the record reached 1.09 and 3.01 times the acceleration of gravity (g), respectively. The SAC algorithm, however, sustained higher record intensities of 1.38 and 4.42, respectively.

The remarkable performance of the SAC algorithm in the fragility curves is evident and in accordance with the performance criteria provided in Table 2. The average peak acceleration threshold for the slight and moderate damage states were nearly equal and perhaps slightly smaller for the SAC algorithm. This likely occurred because the algorithm may not have been required at lower vibrations and the time-wise IDA step was assumed three times larger than the uncontrolled structures.
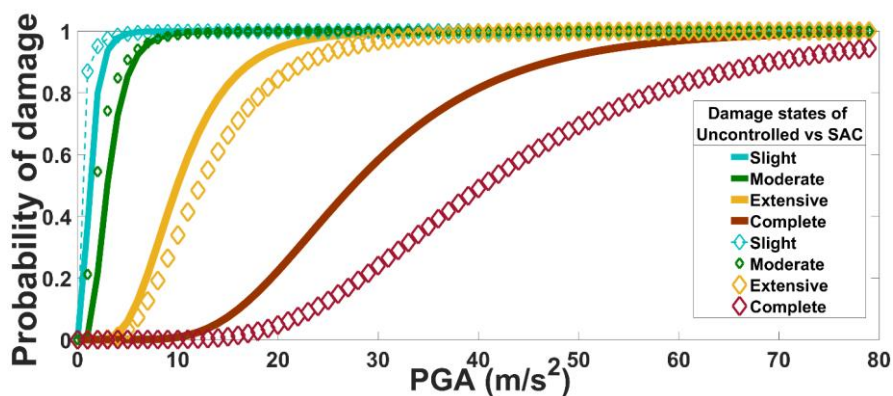

Fig. 9. Fragility curves for slight, moderate and extensive damage states.

To calculate the probability of exceedance of damage states, uncertainties were introduced into the system variables, stiffness mass, and damping coefficient. Next, several series of systems were generated using a log-normal distribution and were subjected to 100 steps of IDA for the 1990 Abbar Manjil records suggested by FEMA P695 at increments of 0.1 g. The mean and standard deviation of the maximum acceleration at the threshold of each damage state was calculated for each series. Fig. 10 shows that the probability of exceeding the extensive and complete damage states were 0.0059 and 0.0036, respectively.
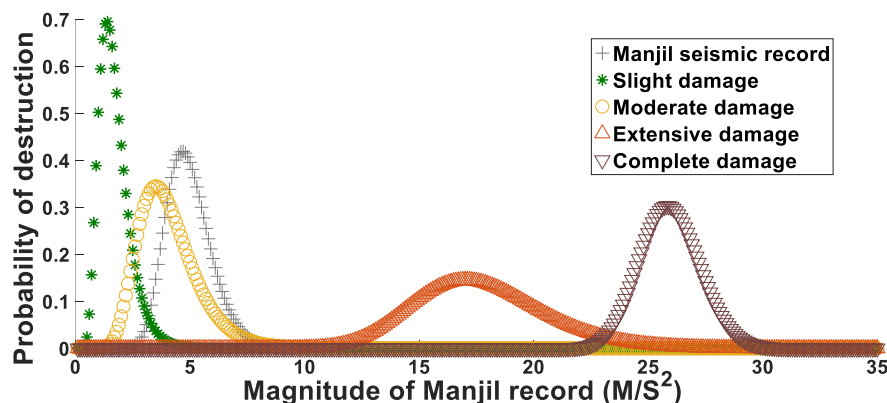

Fig. 10. Probability of being in or exceeding damage states of the 20-story building controlled by SAC.

Conclusion

In this study, the efficiency of three control strategies was investigated for a range of seismic records. The performance criteria revealed that the use of magnetorheological (MR) dampers in high-rise buildings can reduce the seismic response. This reduction was more evident using simple adaptive control (SAC) when the structures were subjected to records of higher intensities and lower probabilities of occurrence. The fragility

9

curves evaluated using the SAC control method sustained higher peak ground accelerations at the threshold of the four damage states compared to uncontrolled structures. This control algorithm follows a reference model with the desired trajectories and obtained a suitable result in the presence of system uncertainty.

Reference

[1]   N. R. Fisco and H. Adeli, "Smart structures: Part I—Active and semi-active control," *Scientia Iranica,* vol. 18, no. 3, pp. 275-284, 2011/06/01/ 2011.

[2]   Y. Lu, "Development of an energy-harvesting magnetorheological fluid damper Development of an Energy-Harvesting Magnetorheological," 2016.

[3]   M. E. Uz and M. N. S. Hadi, "Optimal design of semi active control for adjacent buildings connected by MR damper based on integrated fuzzy logic and multi-objective genetic algorithm," *Engineering Structures,* vol. 69, pp. 135-148, 2014.

[4]   S. Thenozhi and W. Yu, "Advances in modeling and vibration control of building structures," *ANNUAL REVIEWS IN CONTROL,* 2013.

[5]   K. Sobel, H. Kaufman, and L. Mabius, "Implicit Adaptive Control for a Class of MIMO Systems," *IEEE Transactions on Aerospace and Electronic Systems,* vol. AES-18, no. 5, pp. 576-590, 1982.

[6]   I. Barkana, "Simple Adaptive Control: The Optimal Model Reference – Short tutorial," *IFAC Proceedings Volumes,* vol. 46, no. 11, pp. 396-407, 2013/01/01/ 2013.

[7]   I. Bar-Kana and H. Kaufman, "Robust simplified adaptive control for a class of multivariable continuous-time systems," in *1985 24th IEEE Conference on Decision and Control*, 1985, pp. 141-146.

[8]   O. A. S. Al-fahdawi, L. R. Barroso, and R. W. Soares, "Simple adaptive control method for mitigating the seismic responses of coupled adjacent buildings considering parameter variations," *Engineering Structures,* vol. 186, no. February, pp. 369-381, 2019.

[9]   O. A. S. Al-fahdawi, L. R. Barroso, and R. W. Soares, "Semi-active adaptive control for enhancing the seismic performance of nonlinear coupled buildings with smooth hysteretic behavior," *Engineering Structures,* vol. 191, no. November 2018, pp. 536-548, 2019.

[10]   T. Soong, *Active Structural Control: Theory and Practice*. Department of Civil Engineering State University of New York at Buffalo.

[11]   M. Bitaraf, O. E. Ozbulut, S. Hurlebaus, and L. Barroso, "Application of semi-active control strategies for seismic protection of buildings with MR dampers," *Engineering Structures,* vol. 32, no. 10, pp. 3040-3047, 2010.

[12]   I. Barkana and J. Z. Ben-Asher, "Simple Adaptive Control Applications to Large Flexible Structures," *Journal of Guidance, Control, and Dynamics,* vol. 34, no. 6, pp. 1929-1932, 2011/11/01 2011.

[13]   G. Leitmann, "Semiactive Control for Vibration Attenuation," *Journal of Intelligent Material Systems and Structures,* vol. 5, no. 6, pp. 841-846, 1994/11/01 1994.

[14]   B. F. Spencer, S. J. Dyke, M. K. Sain, and J. D. Carlson, "Phenomenological Model for Magnetorheological Dampers," *Journal of Engineering Mechanics,* vol. 123, no. 3, pp. 230-238, 1997/03/01 1997.

[15]   S. Sefidkar-Dezfouli, "Design, Simulation, and Fabrication of a Lightweight Magneto Rheological Damper," SIMON FRASER UNIVERSITY, March 5, 2014

[16]   S. D. Bharti, S. M. Dumne, and M. K. Shrimali, "Seismic response analysis of adjacent buildings connected with MR dampers," *Engineering Structures,* vol. 32, no. 8, pp. 2122-2133, 2010.

[17]   P. G. Somerville, N. Smith, S. Punyamurthula, and J. Sun, "Development of Ground Motion Time Histories for Phase 2 of the FEMA/SAC Steel Project, SACBD-97/04," Sacramento, CA1997.

[18]   B. F. Spencer Jr, S. J. Dyke, and H. S. Deoskar, "Benchmark problems in structural control: part I—Active Mass Driver system," *Earthquake Engineering & Structural Dynamics,* vol. 27, no. 11, pp. 1127-1139, 1998/11/01 1998.

[19]   D. o. H. Security, E. P. Fema, D. Response, and D. C. Mitigation Division Washington, *Multi-hazard Loss Estimation Methodology Earthquake Model HAZUS®MH MR4 Technical Manual*. 2003.

[20]   J. R. Harris *et al.*, "Quantification of Building Seismic Performance Factors," no. June, 2009.

[21]   S. Babaei and P. Zarfam, "Optimization of shape memory alloy braces for concentrically braced steel braced frames," in *Open Engineering* vol. 9, ed, 2019, p. 697.